Advances in Concrete Construction, *Vol. 6, No. 2 (2018) 199-220*
DOI: https://doi.org/10.12989/acc.2018.6.2.199

Effects of sulphuric acid on mechanical and durability properties of ECC confined by FRP fabrics

Mehmet Eren Gülşan[*1], Alaa Mohammedameen[1,2a], Mustafa Şahmaran[3b], Anıl Niş[4c], Radhwan Alzeebaree[1,2d] and Abdulkadir Çevik[1e]

[1]*Department of Civil Engineering, Gaziantep University, Gaziantep, Turkey*
[2]*Department of Civil Engineering, Dohuk Polytechnic University, Dohuk, Iraq*
[3]*Department of Civil Engineering, Hacettepe University, Ankara, Turkey*
[4]*Department of Civil Engineering, İstanbul Gelisim University, Istanbul, Turkey*

(Received February 23, 2018, Revised March 26, 2018, Accepted March 27, 2018)

Abstract. In this study, the effects of sulphuric acid on the mechanical performance and the durability of Engineered Cementitious Composites (ECC) specimens were investigated. The carbon fiber reinforced polymer (CFRP) and basalt fiber reinforced polymer (BFRP) fabrics were used to evaluate the performances of the confined and unconfined ECC specimens under static and cyclic loading in the acidic environment. In addition, the use of CFRP and BFRP fabrics as a rehabilitation technique was also studied for the specimens exposed to the sulphuric acid environment. The polyvinyl alcohol (PVA) fiber with a fraction of 2% was used in the research. Two different PVA-ECC concretes were produced using low lime fly ash (LCFA) and high lime fly ash (HCFA) with the fly ash-to-OPC ratio of 1.2. Unwrapped PVA-ECC specimens were also produced as a reference concrete and all concrete specimens were continuously immersed in 5% sulphuric acid solution (H_2SO_4). The mechanical performance and the durability of specimens were evaluated by means of the visual inspection, weight change, static and cyclic loading, and failure mode. In addition, microscopic changes of the PVA-ECC specimens due to sulphuric acid attack were also assessed using scanning electron microscopy (SEM) to understand the macroscale behavior of the specimens. Results indicated that PVA-ECC specimens produced with low lime fly ash (LCFA) showed superior performance than the specimens produced with high lime fly ash (HCFA) in the acidic environment. In addition, confinement of ECC specimens with BFRP and CFRP fabrics significantly improved compressive strength, ductility, and durability of the specimens. PVA-ECC specimens wrapped with carbon FRP fabric showed better mechanical performance and durability properties than the specimens wrapped with basalt FRP fabric. Both FRP materials can be used as a rehabilitation material in the acidic environment.

Keywords: Engineered Cementitious Composite (ECC); carbon fiber; basalt fiber; polyvinyl alcohol fiber; sulphuric acid attacks

∗Corresponding author, Assistant Professor, E-mail: gulsan@gantep.edu.tr
[a]Ph.D. Student, E-mail: alatroshi2015@gmail.com
[b]Professor, E-mail: sahmaran@hacettepe.edu.tr
[c]Ph.D., E-mail: anis@gelisim.edu.tr
[d]Ph.D. Student, E-mail: alzeebaree@gmail.com
[e]Professor, E-mail: akcevik@gantep.edu.tr

http://www.techno-press.org/?journal=acc&subpage=7 ISSN: 2287-5301 (Print), 2287-531X (Online)

1. Introduction

The durability of the structures under chemical attacks becomes significant especially in urban areas due to high population, increased number of factories and hazardous wastes. Ordinary concrete degradation under chemical attacks is a well-known issue among researchers and ongoing studies continue to prevent the degradation of concrete under chemical attacks. In addition to chemical attacks, structures are subjected to axial load, shear force and bending moment, especially in earthquake zones. In such a situation, structures experience seismic loads after the loss of mechanical strength due to chemical attack and the failure of the structures becomes inevitable.

In recent decades, fiber reinforced polymer (FRP) fabrics have been used to prevent the brittle mode of failure associated with plain concrete and they have involved extensive research for the strengthening of concrete structures (Bakis *et al*. 2002; Hollaway 2001, Hosseinpour and Abbasnia 2014, Teng *et al*. 2002).

International design codes and specifications have been published for the strengthening of concrete structures using externally bonded FRP jacket systems (AC125 1997, ACI Committee 440 2002, FBI 2001, Li 2006, TR 55 2004). The preference of FRP fabrics for the repair and strengthening aims can be attributed to low thermal conductivity, lightweight, high resistance to corrosion and chemical attacks (Halliwell 2010, Hamilton *et al*. 2009, Nanni 1995).

Engineered Cementitious Composite (ECC) is one of the most familiar and effective strain-hardening cementitious composite types. ECC provides high ductility and enables the formation of multiple micro-cracks instead of a single macro crack under uniaxial tensile and flexural loadings, which makes ECC significantly durable under static and cyclic (earthquake) loading compared to conventional concrete. The tensile strain capacity of the ECC concrete can be approximately 300-500 times larger than that of the conventional concrete. In addition, the crack width remains smaller than 60 μm, which prevents or slows down the deterioration rate due to chemical attacks and improves the service life of the structures (Liu *et al*. 2017). ECC has also higher fatigue strength due to the controlled crack propagation of fiber bridging effect (Qiu and Yang 2017).

The usage of fly ash has started to increase due to its environmentally-friendly nature. Fly ash can be used as an aluminosilicate source (Nazari *et al*. 2015) and depending on the source, fly ash is classified as F type (including low CaO) and C type (including more than 20wt.% CaO). Both types of fly ash are naturally low reactive materials and their use improves the durability of the structures (Nazari and Sanjayan 2015). In addition, the durability of structures depends on the environmental factors. The most commonly encountered environmental attacks for concrete structures are temperature fluctuations, wetting-drying, and wind effects (Reis and Ferreira 2006). In addition, the sulphuric acid attack is one of the most hazardous environmental attacks. The effect of acid attacks can arise from different sources, like acid rain, marine environments, or from the soil. Basalt FRP and carbon FRP fabrics showed greater resistance against environmental attacks (Al-tamimi *et al*. 2014, Cai *et al*. 2017, Wu and Li 2017). However, the effect of an acid attack on FRP composites can also occur by a relocation of fluids or moisture. Investigations have shown that the acids can react with the polymer fabrics and they change the chemical composition of FRP. Therefore, deterioration of interfacial transition zone between fibers and matrix is realized, which results in a loss of mechanical performance. Stress corrosion is another common failure type due to acid attack, and it is realized when the internal strength of the material is reduced by acid penetration under sustained internal stress (Kumar *et al*. 2007, Reichhold 2009).

Although there are few studies investigating the acid attack on PVA-ECC specimens, there is

Table 1 Chemical composition and physical properties of F and C type fly ashes and OPC

Materials	CaO	SiO_2	Al_2O_3	Fe_2O_3	MgO	SO_3	K_2O	Na_2O	Loss of Ignition	Specific Gravity	Blain Fineness (m^2/kg)
FA-F (%)	1.568	62.352	21.137	7.847	1.756	0.103	0.726	2.445	2.071	2.300	387
FA-C (%)	15.537	46.946	11.680	7.976	6.505	3.466	3.132	2.327	2.446	2.270	306
OPC (%)	62.584	20.246	5.308	3.037	2.283	2.705	0.615	0.216	3.015	3.150	326

limited or lack of study related to the effect of the sulphuric acid attack on PVA-ECC specimens wrapped with basalt and carbon FRP fabrics under static and cyclic loading. In addition, the use of FRP materials as a rehabilitation material in the acidic environment is also investigated. SEM analysis was conducted to clarify the effect of the acid attack on wrapped and unwrapped PVA-ECC specimens in micro-scale. The obtained outcomes of the study can be important for structures exposed to acid attack and they can be used to improve the service life of structures.

2. Experimental program

2.1 Materials

The used materials in the production of PVA-ECC mixes were F-type fly ash, C-type fly ash, OPC, silica sand, water, high range water reducing admixture and PVA fibers. Table 1 shows the chemical and physical properties of the binder materials.

The polyvinyl alcohol (PVA) fiber with a fraction of 2% was used in the research, which had a diameter of 39 μm and a length of 8 mm. The tensile strength, elastic modulus and maximum elongation of fibers were 1620 MPa, 42.8 GPa, and 6.0%, respectively (Li *et al*. 2002). Research showed that the peak load or stress of unoiled PVA fibers was greater than the oiled PVA fibers due to higher frictional and chemical bond. However, the crack opening was found much smaller, which resulted in decreased energy absorption capacity (Pan *et al*. 2015). It was attributed to the rupture of the unoiled PVA fiber from the matrix instead of pullout of fibers from matrix. During the peak load, unoiled PVA fibers had higher frictional and chemical bond and reached the peak load at small pullout lengths. The unoiled fibers did not completely pull out of the matrix and rupture occurred (Li and Fischer 2002). Therefore, the surfaces of the PVA fibers were oiled with a proprietary hydrophobic oiling agent of 1.2% by weight in order to reduce the frictional and chemical bond and to improve strain hardening performance of PVA-ECC (Sahmaran *et al*. 2007). The increase in the aggregate size had an adverse effect on ductility performance of ECC (Sahmaran *et al*. 2009) and microsilica sand with an average grain size of 110 μm and a maximum grain size of 200 μm used in the study for that reason. Table 2 presents the mix design of the PVA-ECC. The ratio of fly ash to OPC and the ratio of micro silica sand to the binder were selected as 1.2 and 0.36 by weight, respectively. Research indicated that water to binder ratio of 0.3 was the balance value for both strain hardening behavior (improved toughness) of ECC and good fiber dispersion resulting from the high rheological behavior (Meng *et al*. 2017). Therefore, the water to binder ratio was chosen as 0.27 in this study, which was below the indicated balance point value and it was expected to perform improved strain hardening response. High range water reducing admixture was also added to the PVA-ECC mixes until the desired fresh properties of PVA-ECC mixes were obtained as specified by a previous study (Yang *et al*. 2009). As a result, two mixes

Table 2 Typical mix design of PVA-ECC specimens

Cement	Water	Microsilica	Fly Ash	HRWRA*	Fiber (%)
1	0.56	0.80	1.20	0.013	2.00

HRWRA* = High range water reducing admixture; all ingredients proportion, by weight, except for fiber.

Table 3 The properties of fabric sheets

FRP types	Tensile Strength (MPa)	Modulus of Elasticity (GPa)	Elongation (%)	Thickness (mm)	Area Weight (g/m^2)
BFRP	2100	105	2.6	0.3	300
CFRP	4900	240	2	0.3	300

Table 4 The properties of fabric sheets

FRP types	Pot life at 20℃ (Min)	Flexural Strength 7 days (N/mm^2)	Compressive Strength 7 days (N/mm^2)	Bond Strength 7 days (N/mm^2)	Mixing ratio	Modulus of Elasticity 7 days (GPa)	Fluid density (kg/lt)
Teknobond 300 Tix	30	≥25	≥62.5	≥3	4:1	>20	1,02±0,02

were obtained as the LCFA-ECC mix (produced with low calcium F-type fly ash) and the HCFA-ECC mix (produced with high calcium C-type fly ash).

In this study, PVA-ECC specimens were confined by using uni-directional carbon fiber reinforced polymer (CFRP) and basalt fiber reinforced polymer (BFRP) fabrics to observe the durability and mechanical performance of these materials under sulphuric acid attack. Table 3 presents the mechanical and physical properties of the FRP materials. An epoxy-based adhesive, Teknobond 300 Tix, was used and its general properties were given in Table 4. The application of the epoxy-based adhesive to the PVA-ECC specimens was realized according to the user guide of the technical document

2.2 Specimen preparation and curing condition

Cylinder specimens with dimensions of 100 mm in diameter and 200 mm in length were prepared to measure compressive strength of PVA-ECC specimens. After 24 hours, specimens were demolded and cured in a water tank for 28 days at 23±2℃. Then specimens were left in an ambient condition for drying. After required strength, carbon and basalt FRP wrappings were realized on certain specimens according to the FRP application procedure as shown in Fig. 1.

In the first stage, concrete surfaces were prepared by eliminating the residual powders with a wire brush and cleaning the surface by an air compressor. In the second stage, FRP fabrics were prepared by cutting each of the sheets with a length of 115 cm (three-layer continuous wrapping length with an overlap of 15 cm between layers) and width of 19 cm (cylinder height minus 0.5 cm at both top and bottom sides to prevent axial load on FRP). In the final stage, implementation of FRP fabrics was realized by coating inner sides of the FRP fabrics with epoxy resin. Later, specimens were placed inside of the FRP fabrics, then three layers wrapping of the specimens were applied with epoxy resin. In the FRP application procedure, the surface of the specimens was also covered with epoxy resin to fill the pores on the surface and to obtain a perfect bond between concrete and FRP fabrics. In addition, the orientation of fibers of FRP fabrics was taken into

(a) Specimen surface preparation

(b) Application of FRP fabrics

Fig. 1 Main steps of applying FRP fabric

consideration during the covering process to ensure alignment of fibers perpendicular to the axial direction of loading. For the outermost layers of FRP fabrics, 15 cm overlap length was provided to obtain a perfect bond between FRP layers and to prevent slippage of FRP layers. Separation of fibers from the edge of FRP sheets was prevented during wrapping process to prevent premature failure of the specimens. After FRP installation, specimens were left in the ambient environment for 7 days to obtain the required strength of the epoxy resins.

2.3 Specimens for mechanical tests

As a result of the FRP installation procedure, three types of specimens; control (without wrapping), and specimens wrapped with carbon FRP and specimens wrapped with basalt FRP, were obtained. In addition, two mixes; LCFA-ECC mix and HCFA-ECC mix were produced. Specimens were left under two different environments; sulphuric acid environment and control environment (unexposed specimens). Control specimens (unexposed specimens) were tested at the ages of 28 days and 90 days, while specimens exposed to the sulphuric acid environment were tested at the age of 90 days. (28 days curing regime and the remaining days under sulphuric acid environment). 18 control specimens (6 unwrapped+6 wrapped with carbon CFRP+6 wrapped with BFRP) were tested at the age of 28 days, 36 control specimens (6 unwrapped+static loading, 6

unwrapped+cyclic loading, 6 CFRP+static loading, 6 CFRP+cyclic loading, 6 BFRP+static loading, 6 BFRP+cyclic loading) were tested at the age of 90 days. For specimens exposed to sulphuric acid attack, 24 unwrapped specimens (6 unwrapped+static loading, 6 unwrapped+cyclic loading, 6 unwrapped+then wrapped (after acid exposure)+static loading, 6 unwrapped+then wrapped (after acid exposure)+cyclic loading) and 24 wrapped specimens (6 CFRP+static loading, 6 CFRP+cyclic loading, 6 BFRP+static loading, 6 BFRP+cyclic loading) were produced and as a total 48 specimens were tested at the age of 90 days under acid attack. It should be noted that 12 unwrapped specimens exposed to sulphuric acid attack were later wrapped with FRP fabrics to investigate the performances of FRP as rehabilitation/retrofit materials.

2.4 Specimens under sulphuric acid attack

There is no standard test method available to evaluate the resistance of concretes under chemical attack. ASTM C 267 test method (ASTM C267-01 2012) recommends that specimens should be soaked in water for 24 hours to obtain water saturated specimens prior to chemical attacks.

Therefore, specimens were immersed in water for 24 hours and initial saturated weights of the specimens were recorded. Then specimens were soaked in 5% sulphuric acid for a period of two months. At the same time, control specimens for each different concrete were left in ambient condition at a room temperature of 23±2℃ in the laboratory for two months for comparison. After the end of each week, PVA-ECC specimens were taken from the acid solution, chemical reaction products on the concrete surface were cleaned by water. Then the specimens were left to drying under laboratory conditions at temperatures of 23±2℃ for 2 hours prior to weight measurements of the specimens.

2.5 Testing procedure

Compressive strength tests were carried out on cylinder specimens with a diameter of 100 mm and length of 200 mm under static and cyclic loadings. Compressive strength tests were carried out according to ASTM C39 (ASTM C39/C39M-12 2012). All compressive strength tests were performed under displacement-controlled loading with a rate of 0.2 mm/min. Two linear variable displacement transducers (LVDT) were attached to measure axial deformations in the specimens as shown in Fig. 2. Stress and strain data were obtained for each specimen.

3. Experimental results and discussion

3.1 Visual inspection

Fig. 3 illustrates the specimens exposed to 5% sulphuric acid solutions for 15 days, one month and two months, respectively. The surface color of the high lime containing fly ash specimens (HCFA) changed from grey to white after 15 days of exposure, while the surface color of the low lime fly ash specimens (LCFA) remained grey even after two months of exposure. For HCFA specimens, white layer gypsum crystals were formed and the amount of the gypsum crystals increased with an increase in the exposure time, which resulted in higher deterioration on the concrete surfaces as shown in Fig. 3. Moderate surface erosions and some small cracks were

Fig. 2 Specimen under axial load

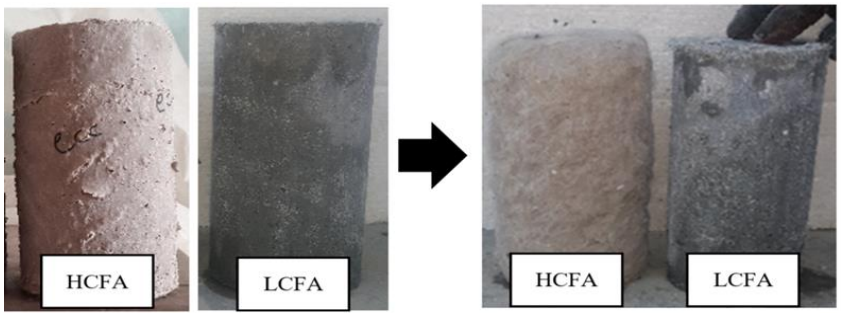

(a) After 15 days of chemical exposure (b) After one month of chemical exposure

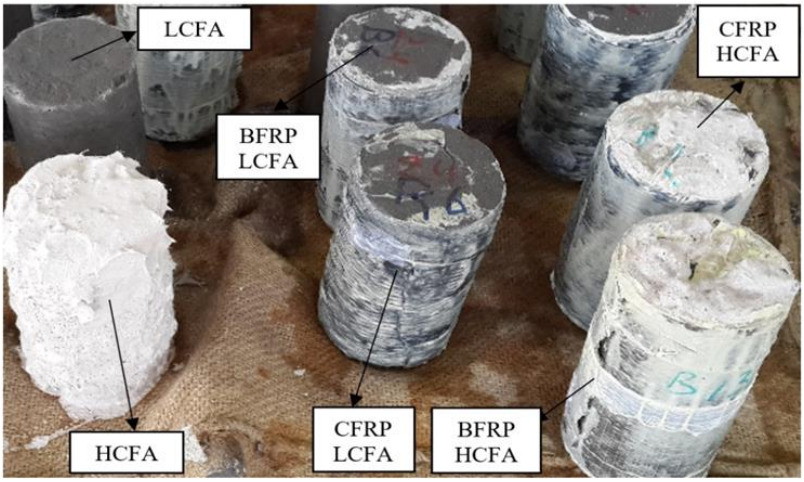

(c) After two months of chemical exposure

Fig. 3 Deterioration of specimens under sulphuric acid environment

observed on LCFA specimen surface without color change. It was also visually observed that more lateral expansion occurred on HCFA specimens than LCFA specimens, which may be attributed to higher gypsum and ettringite formation due to high CaO content on HCFA specimens. When the outer surface colors of specimens confined with basalt and carbon FRP were compared, the colors

of both specimens changed to white and most deterioration (most whiter one) was observed on basalt FRP specimens than carbon FRP specimens under sulphuric acid attack, as shown in Fig. 3.

PVA fibers were also deteriorated by spillage of fibers due to surface erosions exposed to sulphuric acid solutions. When specimens were investigated in details, PVA fibers of HCFA specimens deteriorated more severe than PVA fibers of LCFA specimens. PVA fiber deterioration was also observed on specimens wrapped with basalt and carbon FRP. However, in this case, PVA fiber deterioration was only observed at the bottom and top parts of the cylinder specimens (unwrapped part of the specimens). Due to the confinement in the lateral direction, PVA fiber deterioration was not observed.

Wallah and Rangan (2006) studied the effect of 2% sulphuric acid attack on geopolymer concrete and found out that sulphuric acid damage was observed only in the 20 mm outer side of the cylinder concrete, which had a 100 mm diameter. In this study, slices of the cylinder concrete exposed to the sulphuric acid solution were also investigated and similar observations were obtained with the previous study (Wallah and Rangan 2006). Acid penetration was observed at the 8 mm outer part of the cylinder specimens, and the remaining inner parts were found unexposed as shown in Fig. 4. It was clearly observed that the acid damage in HCFA specimens was found more severe than LCFA specimens. This result was also supported by the earlier investigation, which stated that the acid attack is a surface phenomenon and the deterioration begins at the surface and progresses inside of the concrete (Emmanuel *et al*.1988). In addition, SEM observations were also

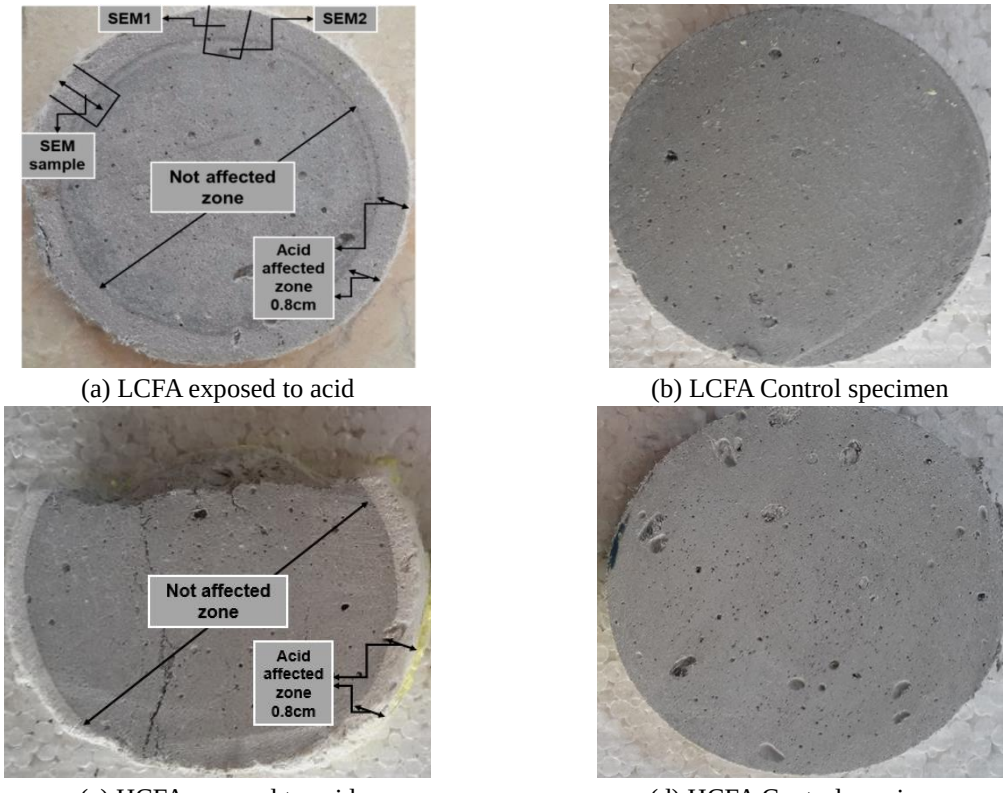

(a) LCFA exposed to acid (b) LCFA Control specimen

(c) HCFA exposed to acid (d) HCFA Control specimen

Fig. 4 ECC cylinder specimen slice showing acid affected zone

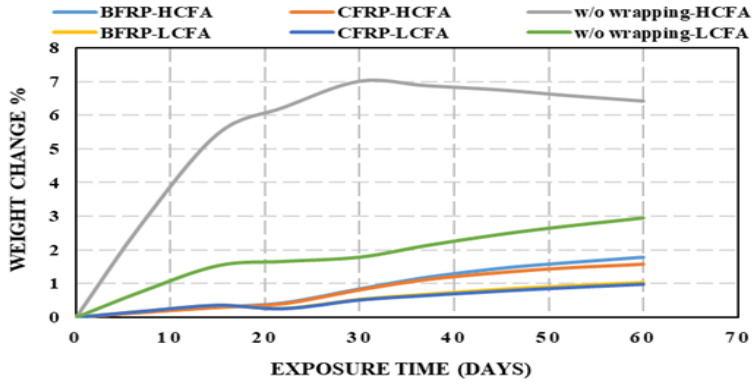

Fig. 5 Weight change in ECC specimen exposed to acid attack for duration 60 days

realized at the acid affected and unaffected zones, as shown in Fig. 4.

3.1 Weight change

Specimen weights were measured under two months of chemical exposure and weight change (%) of the specimens were given in Fig. 5. Results showed that all specimens showed weight gain under sulphuric acid solution absorption, and highest weight increase was observed on specimens without wrapping. The gained weights were 6.4% for HCFA specimens and 3% for LCFA specimens. For wrapped specimens, HCFA specimens also showed slightly higher weight gain than the LCFA specimens. In addition, LCFA specimens confined with carbon FRP showed the least weight gain and therefore, LCFA specimens with CFRP fabrics showed slightly better chemical resistance than BFRP fabrics under acid attack. Lower weight gains result of LCFA specimens with/out FRP wrapping may be attributed to the higher fineness ratio, which resulted in reduced porosity and decreased solution absorption. Weight gain due to acid exposure was also reported in the earlier research (Al-Dulaijan *et al*. 2007; Thokchom 2014). In addition, HCFA specimens without wrapping showed weight loss (deterioration) after one month of exposure, which could be resulted from both alkali and some material dissolution from concretes into the acidic medium (Thokchom 2014). The formation of gypsum and ettringite due to the reactions between chemical solution and cement caused increased volume by a factor of about two (Soroka 1979) and reduced density of concrete. Therefore, initial weight gains of the specimens may result from the lower reduction amount in relative density than the increase in relative volume (Attiogbe *et al*. 1988).

3.3 Compressive strengths of the specimens

In general, the performances of PVA - ECC specimens wrapped with FRP under axial load were found to be consistent with the behavior of FRP confined concrete in the literature. During early stages of compression loading, the noise associated with the microcracking of ECC concrete was obvious, which represented the initiation of the stress transfer from the expanded ECC concrete to the FRP fabrics. The intensity of the cracking noises could be heard prior to the failure that realized after the rupture of FRP fabrics slowly with a sudden and violent noise. Failure of the FRP fabrics started from an overlap area of the fabrics at the middle height and progressed to the top

Table 5 Compressive strength of LCFA and HCFA specimens

Compressive Strength of LCFA - ECC specimens (MPa)											
STA	Control 28 days			Control 90 days			Exposed to Acid Attack				
	w/o wrap	CFRP	BFRP	w/o wrap	CFRP	BFRP	w/o wrap	CFRP	BFRP	CFRP-A*	BFRP-A*
AVG	21.6	60.6	43.3	27.5	75.4	53.6	20.8	72.5	50.4	66.4	47.0
SD	0.90	0.69	0.89	0.70	0.63	0.79	0.70	0.53	0.57	0.89	1.11
Compressive Strength of HCFA - ECC specimens (MPa)											
STA	Control 28 days			Control 90 days			Exposed to Acid Attack				
	w/o wrap	CFRP	BFRP	w/o wrap	CFRP	BFRP	w/o wrap	CFRP	BFRP	CFRP-A*	BFRP-A*
AVG	47.6	73.2	56.7	57.3	91.0	68.1	36.8	79.5	58.2	70.1	51.1
SD	0.65	0.57	0.60	0.74	1.00	0.76	0.85	0.54	0.61	0.80	1.00

CFRP-A* and BFRP-A*=The specimens wrapped after exposed to acid by CFRP and BFRP respectively.

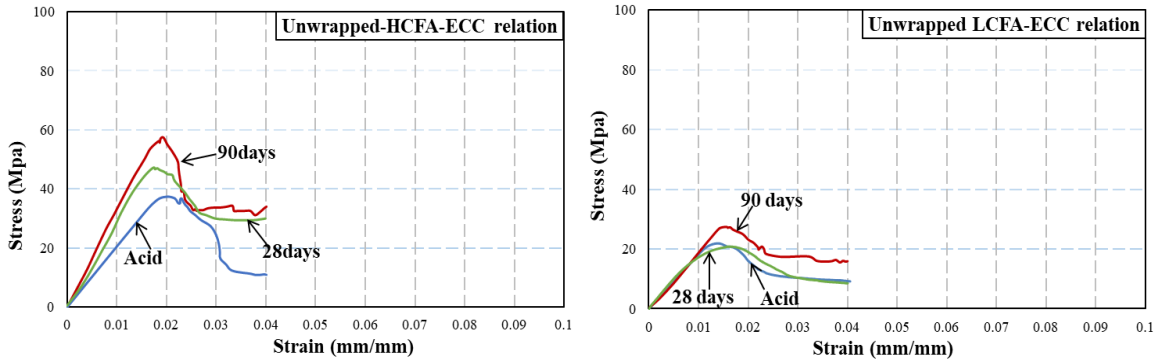

(a) Unwrapped HCFA-ECC specimens (b) Unwrapped LCFA-ECC specimens

Fig. 6 Stress-strain curves of unwrapped ECC specimens

and bottom of the specimens. For the tested specimens, no de-bonding observed in wrapped specimens and all failures occurred due to the rupture of FRP fabrics followed by a ductile behavior of ECC. Table 5 illustrates the both average compressive strengths (AVG) and standard deviations (SD) of the specimens. Results indicated that FRP wrapped specimens showed superior performance than unwrapped specimens under both ambient and acid environments.

3.3.1 Compressive behavior of unwrapped specimens

Fig. 6 shows the typical compressive stress-strain curves of unwrapped PVA-ECC specimens. Results indicated that compressive strength of unwrapped compressive specimens increased up to 90 days. The increase in the compressive strength can be attributed to the continuous hydration reactions and the slow pozzolanic reaction of fly ash. Similar investigations were also reported in the previous studies (Liu *et al*. 2017, Zhigang and Zhang 2017).

The compressive strength values of 90-day curing specimens were 20.3% and 27.2% higher than the 28- day strengths of LCFA specimens at later ages was expected due to lower CaO content in the low lime fly ash particles as the rate of hydration reactions was slow, in which strength

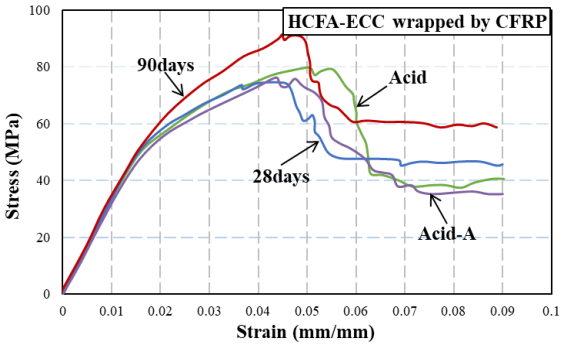

(a) HCFA-ECC specimen wrapped by CFRP

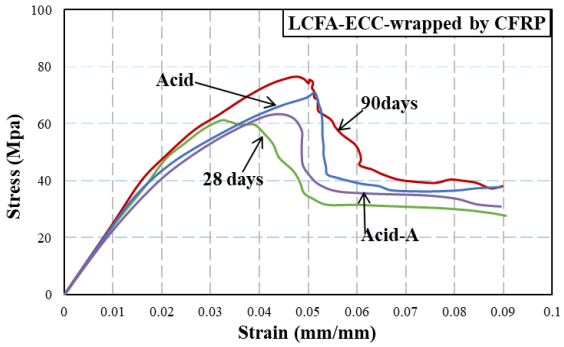

(b) LCFA-ECC specimen wrapped by CFRP

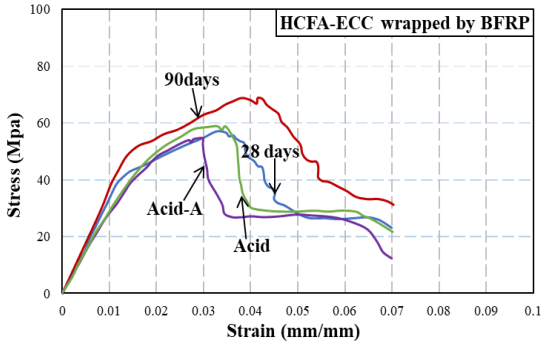

(c) HCFA-ECC specimen wrapped by BFRP

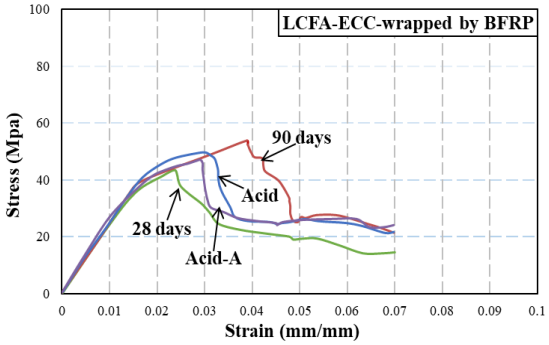

(d) LCFA-ECC specimens wrapped by BFRP

Fig. 7 Stress-strain curves of CFRP and BFRP wrapped ECC specimen

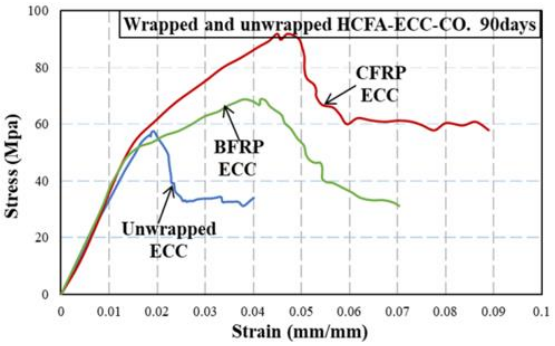

(a) HCFA specimens

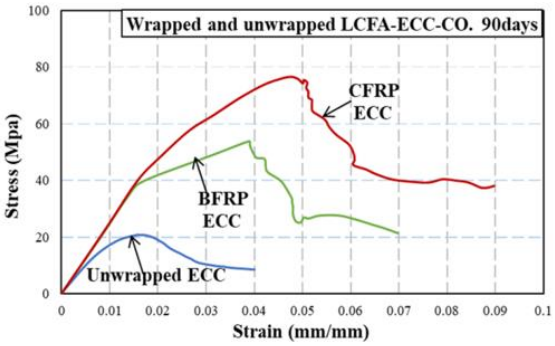

(b) LCFA specimens

Fig. 8 Stress-strain curves of wrapped and unwrapped PVA- ECC specimens

development (C_3S and C_2S production) became time dependent. Reductions in strength due to sulphuric acid attack were 22.7% and 4% for 28-days, 35.7% and 24.4% for 90-days strengths of HCFA and LCFA specimens, respectively. Higher strength reduction for HCFA specimens may be also attributed to high CaO amount in the HCFA specimens.

3.3.2 Compressive behavior of wrapped specimens

Fig. 7 represents the compressive behavior of wrapped PVA-ECC specimens. The results

showed significant compressive strength increase (more than 2-3 times) when compared to unwrapped specimens. In general, when the outermost FRP fiber ruptured, the compressive load reduced suddenly and then the load began to increase or remain constant due to stress transfer from FRP fabrics to PVA-ECC concrete until the failure of inner FRP fibers and PVA fibers inside the ECC matrix (Li *et al*. 2002).

Similar to unwrapped specimens, compressive strengths of the wrapped specimens also enhanced from 28-days to 90-days. The amounts of enhancement were 24.3% and 20.3% for HCFA specimens and 24.4% and 23.7% for LCFA specimens wrapped with CFRP and BFRP fabrics, respectively. It can be concluded that the effect of concrete matrix on compressive strength was also significant when FRP fibers were also available.

Compressive strengths of the wrapped specimens exposed to the acid solution at the age of 90-days were found higher than the 28-day compressive strengths of the wrapped ones. The amount of increase was found to be 19.6% and 16.4% for the LCFA-ECC specimens and 8.6% and 2.8% for the HCFA-ECC specimens wrapped with CFRP and BFRP fabrics, respectively. This lower increase in the HCFA specimens can be attributed to the deterioration effect of CaO content especially for the high lime fly ash including specimens. In addition, the strengths of the wrapped specimens under acid attack were lower than the unexposed specimens at the age of 90-days, as expected. The reduction amounts due to acid attacks were 12.6% and 14.5% for HCFA specimens and 5.94% and 7.36% for LCFA specimens wrapped with CFRP and BFRP fabrics, respectively.

In the study, unwrapped specimens were exposed to acid attack and then the installations of FRP fabrics were realized on the same specimens in order to find out the effect of FRP materials as rehabilitation/retrofit materials. Results showed that compressive strength of the after wrapped specimens (shown as Acid-A on Figures and CFRP-A and BFRP-A on Table 5) were lower than the before wrapped specimens under acid attack, as expected. The reduction amounts only were 12% and 12.3% for LCFA specimens and 23% and 25% for HCFA specimens wrapped with CFRP and BFRP, respectively. Results indicated that both FRP installation can be also a solution to acid affected concrete and FRP fabrics can be used as a retrofit or rehabilitation material under acid attack.

In addition to compressive strength, ductility was also increased as a result of the FRP wrappings of the specimens. The increase in ductility was reported in the literature for ordinary concrete wrapped with FRP (Mesbah and Benzaid 2017, Photiou *et al*. 2006). ECC specimens generally show strain hardening response, which resulted in an increased ductility and toughness. In addition, FRP wrappings also enhance the ductile behavior. The FRP wrapped ECC specimens showed very high lateral displacement capacities and toughness, especially for the post-peak curve of the stress-strain curve, which makes FRP-ECC specimens essential in structural elements requires high strength and ductility. In the study, basalt and carbon FRP fabrics increased the strain from 0.04 to 0.07 and 0.04 to 0.09, respectively as shown in Figs. 7 and 8. The obtained higher strength and strain resulted from the confinement effect of FRP fibers, which create a triaxial state of the stress along the concrete specimen height. After FRP rupture, PVA-ECC concrete continued to carry the load until the failure of PVA fibers. Specimens wrapped with carbon FRP fabrics showed superior performance than the specimens wrapped with basalt FRP fabrics, and the poor performance was obtained in the unwrapped specimens as shown in Fig. 8.

3.3.3 Failure modes of specimens under compression load

During compression load, expansion of concrete expected on cylinder specimens and both PVA fibers and FRP fabrics resisted the expansion and created a confinement in the circumferential

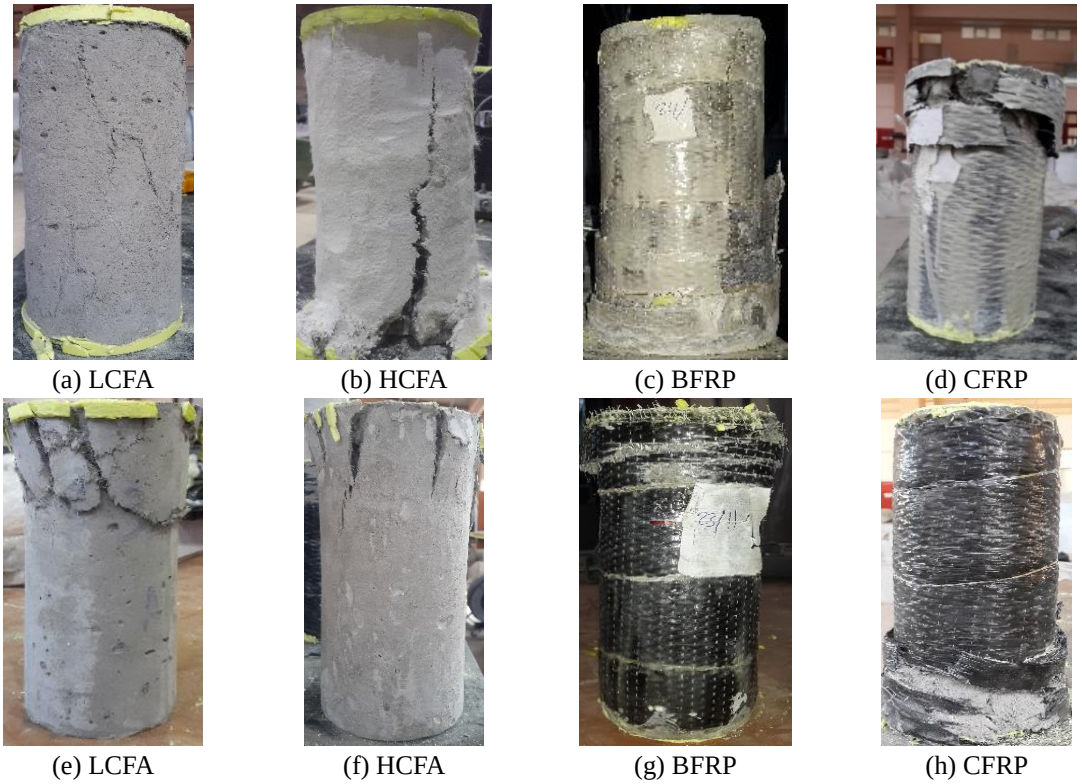

(a) LCFA (b) HCFA (c) BFRP (d) CFRP

(e) LCFA (f) HCFA (g) BFRP (h) CFRP

Fig. 9 Failure mode of PVA-ECC specimens under acid (a,b,c,d) and under ambient (e,f,g,h) environments

direction of the cylinder specimens. When tensile stresses due to axial load exceed the FRP-ECC matrix composite tensile strength resistance, FRP rupture occurred and ECC matrix continued to carry the axial load until the failure of the PVA fibers.

In the study, all failure mechanism realized first FRP rupture and then the failure of PVA-ECC matrix. However, the failure due to poor vertical lap joints had rarely been reported by some studies (Nanni and Bradford 1995, Demers and Neale 1994).

Fig. 9 shows the fracture or failure shapes of the specimens. The crack formation started around the top or bottom region of the specimen and crack openings progressed until the failure at these locations due to high-stress concentrations caused by the friction between the machine plates and the specimen. Since FRP fabrics oriented uni-directional, sudden rupture of the FRP fabrics was realized due to FRP fabrics rupture and hence stress transfer cannot be possible between FRP fibers. During various stages of tests, small popping noises were heard as stated previous studies (Chaallal *et al*. 2003, Chakrabortty and Khennane 2014, Lau and Zhou 2001, Taghia and Bakar 2013). It was clearly observed that the failure of the most of the specimens occurred at the top or bottom region of the specimen when the FRP fabrics were taken off upon specimen failure.

Failure of the unwrapped ECC specimens occurred more violent than the specimens wrapped with FRP fabrics. Due to the high bond strength of PVA fibers, the formed cracks cannot propagate into the mid-lengths of the specimens in general (Li *et al*. 2002). The failure of the unwrapped specimens occurred near the top and bottom of the specimens as similar to the wrapped ones. However, failure of the specimens subjected to acid became under axial or shear failure as shown

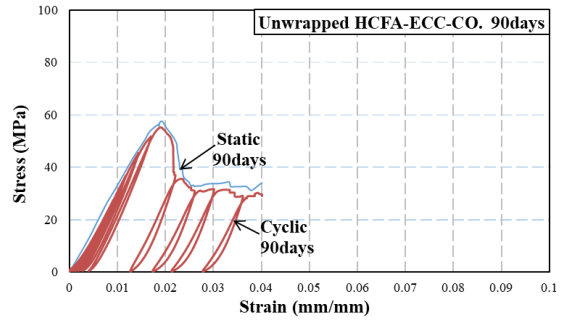

(a) Unwrapped HCFA control specimen (90 days)

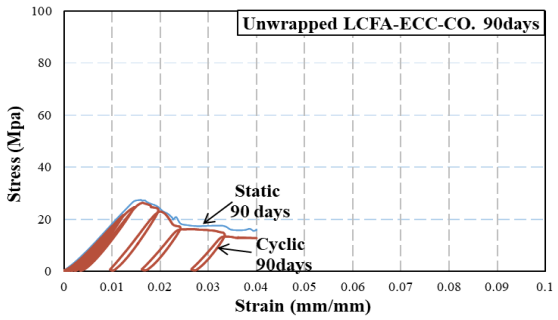

(b) Unwrapped LCFA control specimen (90 days)

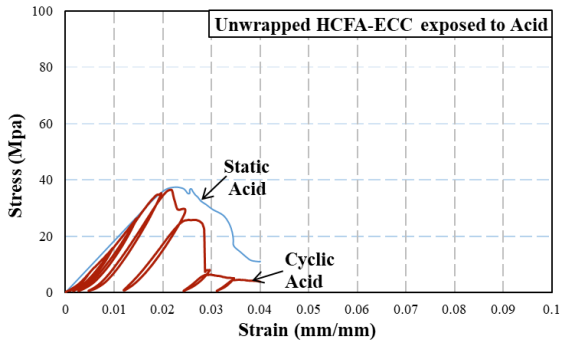

(c) Unwrapped HCFA specimen exposed to acid

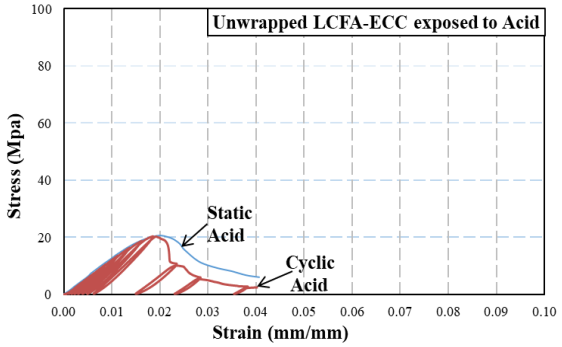

(d) Unwrapped LCFA specimen exposed to acid

Fig. 10 Static and cyclic loading diagrams of unwrapped ECC specimens

in Fig. 9. This may result from gypsum and ettringite formation at the outer surface (~ 1 cm) under sulphuric acid environment. The sulphuric acid created additional tensile stresses and caused defects in the concretes. When the acid effect combined with the external axial load, the cracking may occur at the weakest defects and further elongate along the specimen heights.

3.4 Cyclic loading

Figs. 10 and 11 illustrate the axial stress-strain curves of the tested specimens under both static and cyclic loading. The pre-peak behavior of unwrapped specimens under static and cyclic loading was found almost linear until the peak loads even for the specimens exposed to acid attack, Fig. 10. However, for the post-peak behavior of unwrapped specimens under acid attack, the static and cyclic curve separated from each other, which may be resulted from the further decrease in elastic modulus due to the softening and decreased rigidity of specimens with increasing loading/unloading cycles. This result can be observed especially for HCFA specimens due to high CaO content.

For wrapped specimens, the pre-peak behavior of wrapped specimens assumed as linear until the points that correspond to the failure of unwrapped ones, Fig. 11. After that (at higher stresses), the elastic modulus of PVA-ECC composite decreased due to the cracks occurred in the concrete matrix. However, higher stresses were attained due to the existence of the FRP fabrics. In the post-peak curve, similar stress relaxation was also observed for both static and cyclic loading. It may be attributed to the elastic behavior of the FRP, which improved the resistance of the specimens under

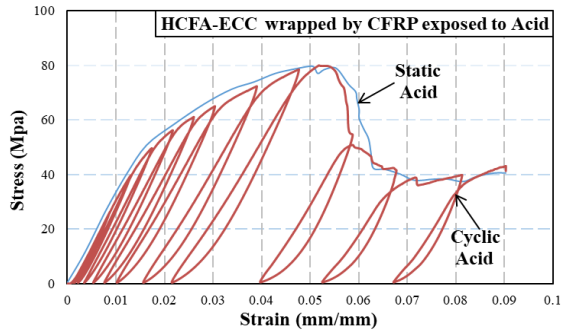

(c) HCFA-CFRP specimen exposed to acid

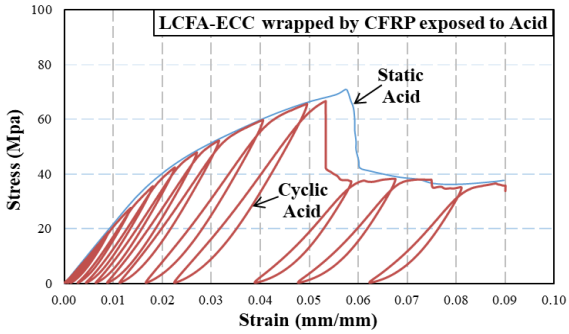

(d) LCFA-CFRP specimen exposed to acid

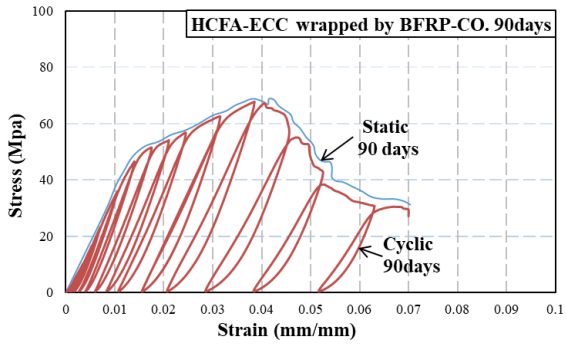

(e) HCFA-BFRP Control specimen 90days

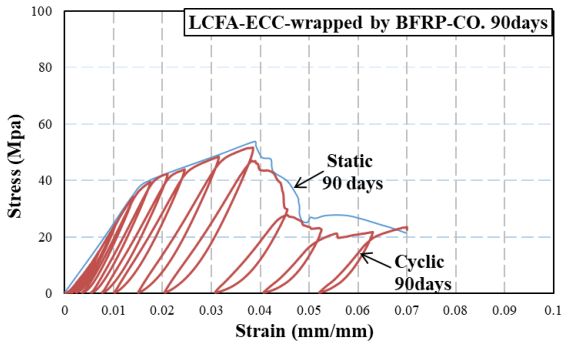

(f) LCFA-BFRP Control specimen 90days

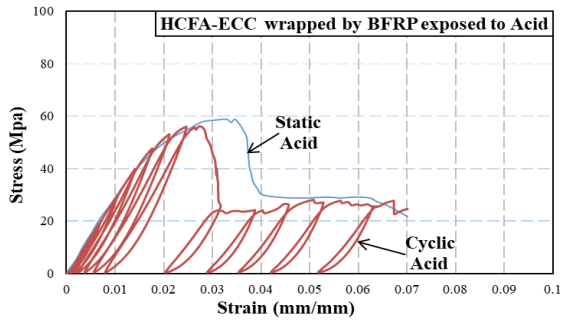

(g) HCFA-BFRP specimen exposed to acid

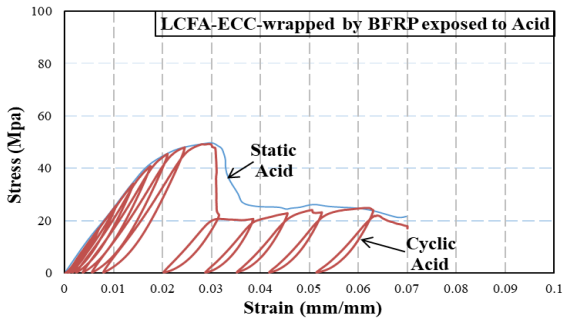

(h) LCFA-BFRP specimen exposed to acid

Fig. 11 Static and cyclic loading diagrams for wrapped ECC specimens

cyclic loadings. The favorable effect of carbon and basalt FRP material on the post-peak curve can be easily observed under acid attack.

The envelopes of all stress-strain curves of ECC-specimens under cyclic loading can be attained by connecting the peaks of the unloading cycles (envelope curve) on the stress-strain curves and the obtained curve matches well with the stress-strain curve of the specimens under static loading. Similar observations were also reported by previous studies (Lam *et al*. 2006, Shah *et al*. 1983) and they also stated that this is also valid for concretes that confined by FRP. In this study, the cyclic and static curves of specimens confined by basalt FRP and carbon FRP complied with each other as shown in Fig. 11. The similar findings were also observed in previous studies (Lam *et al*. 2006, Shah *et al*. 1983, Theodoros 2001).

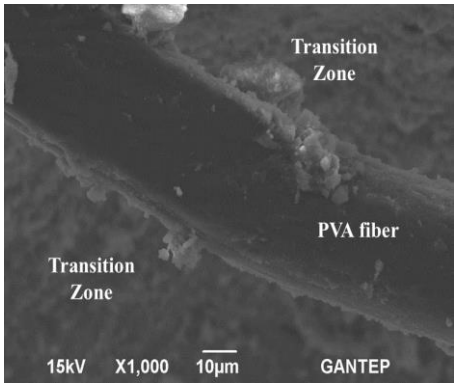

(a) HCFA-ECC control specimens

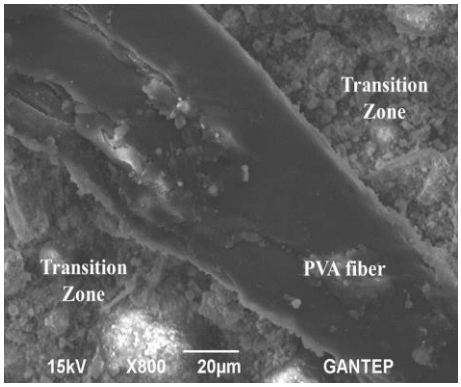

(b) LCFA-ECC control specimens

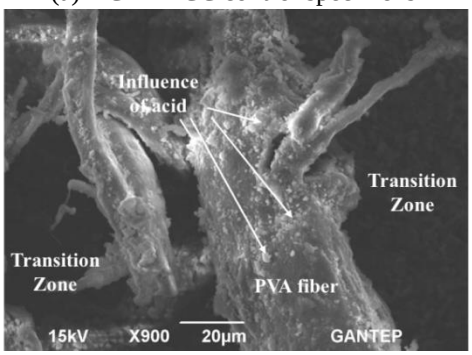

(c) HCFA-ECC exposed to acid (0.8 cm)

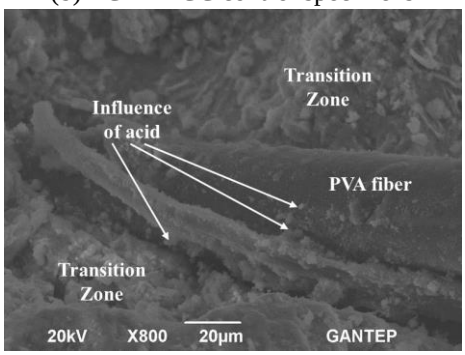

(d) LCFA-ECC exposed to acid (0.8cm)

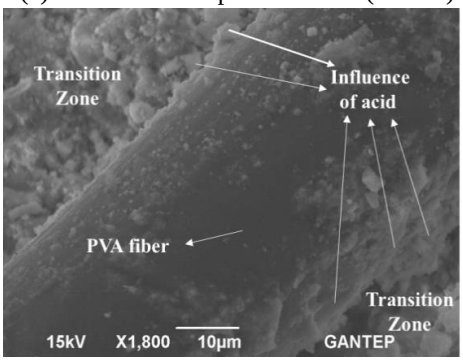

(e) HCFA-ECC exposed to acid (A-1cm)

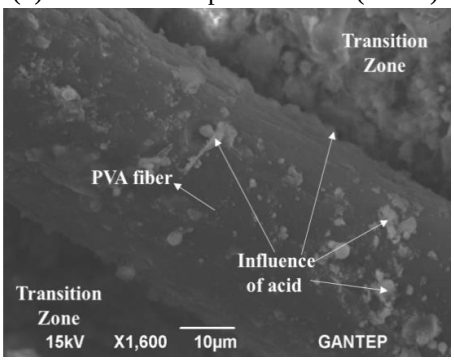

(f) LCFA-ECC exposed to acid (A-1cm)

Fig. 12 SEM pictures of HCFA (left) and LCFA (right)-ECC specimens without wrapping

3.5 Scanning Electron Microscopy (SEM)

Wrapped and unwrapped PVA-ECC samples were analyzed in details by scanning electron microscopy (SEM) to observe changes in the surface of PVA fibers and the interfacial transition zone between the fiber and the matrix. In addition, the changes on the surfaces of basalt and carbon FRP fabrics were investigated in microscale. One inch (2.54 cm) slices of the specimens were cut and discarded from both top and bottom regions and 1 cm thick circular slice from the middle sections of the specimens was used for SEM analysis. The width of the acid affected zone

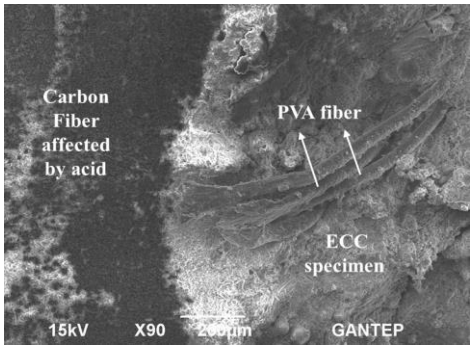

(a) ECC-CFRP exposed to acid (0-1 cm)

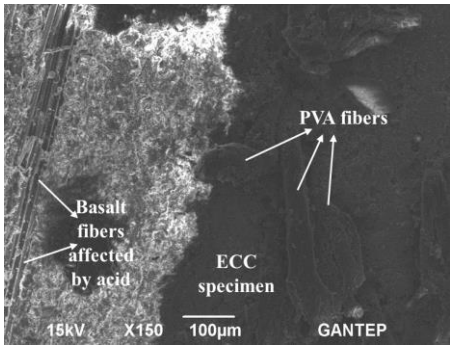

(b) ECC-BFRP exposed to acid (0-1 cm)

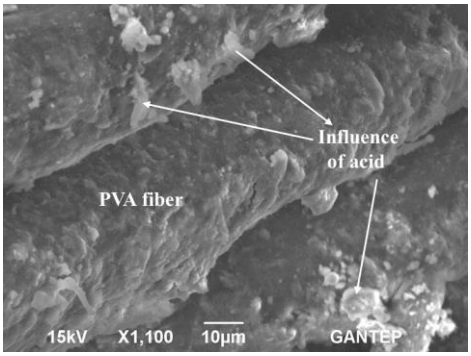

(c) ECC-CFRP exposed to acid (0-1 cm)

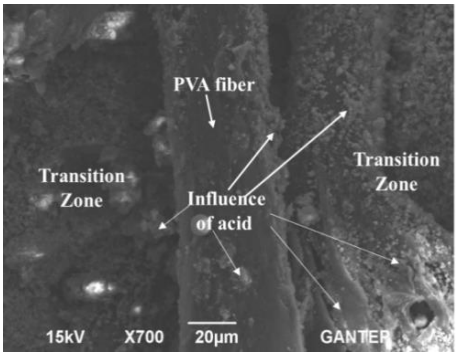

(d) ECC-BFRP exposed to acid (0-1 cm)

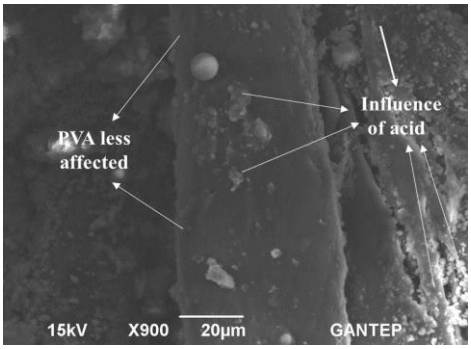

(e) ECC-CFRP exposed to acid (A-1cm)

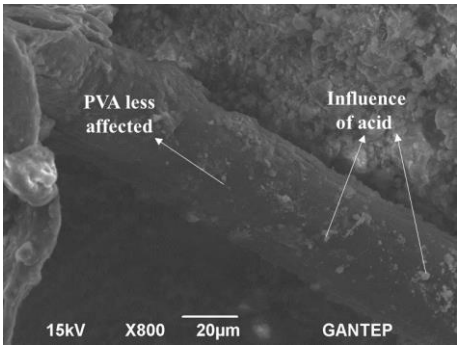

(f) ECC-BFRP exposed to acid (A-1cm)

Fig. 13 SEM pictures of CFRP and BFRP wrapped HCFA specimens

was about 8 mm from the outer layer of the cylinder specimen as shown in Fig. 4. Therefore, two SEM photos were taken for each specimen, one of them was taken at the acid affected zone (0-1 cm from the surface) and the other one was taken from the unaffected zone (close to the affected zone but out of the 1 cm outer layer).

Fig. 12 illustrates the SEM images of the ECC specimens without wrapping under different environments. The white deposits composed on the surface of the PVA fibers and the number of white deposits was higher especially for HCFA specimens than LCFA specimens. Due to the high calcium content, Ca/Si ratio becomes higher and the free calcium results in deterioration of the cement paste. In addition, the formation of gypsum and ettringite can cause expansion,

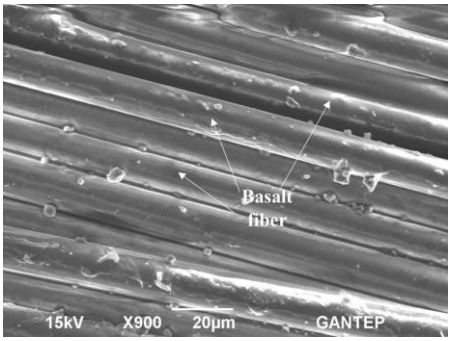

(a) BFRP (w/o epoxy) control specimen

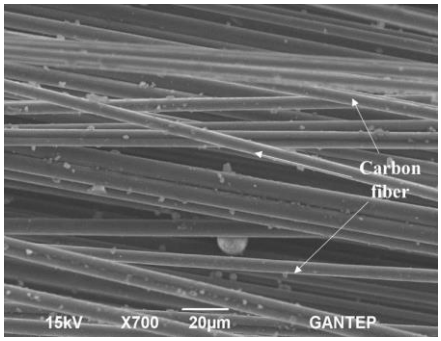

(b) CFRP (w/o epoxy) control specimen

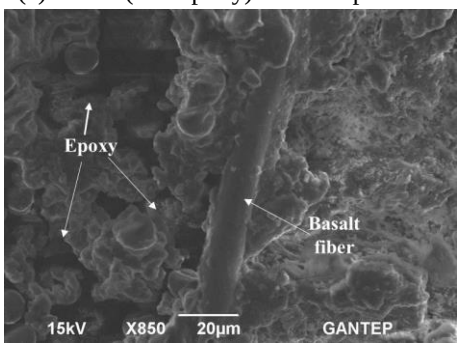

(c) BFRP-epoxy control specimen

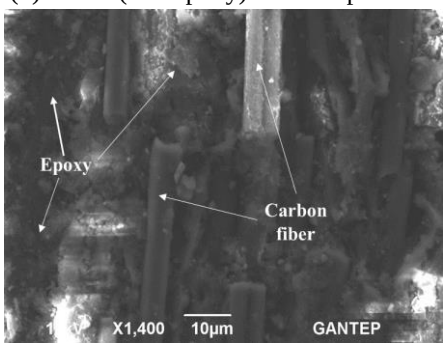

(d) CFRP-epoxy control specimen

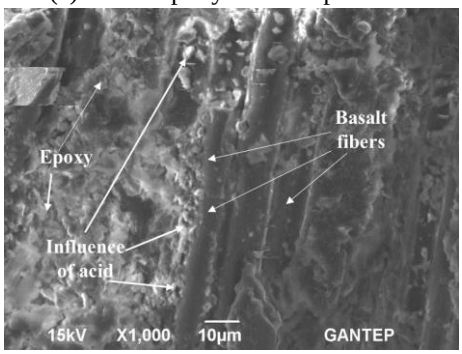

(e) BFRP-epoxy exposed to acid

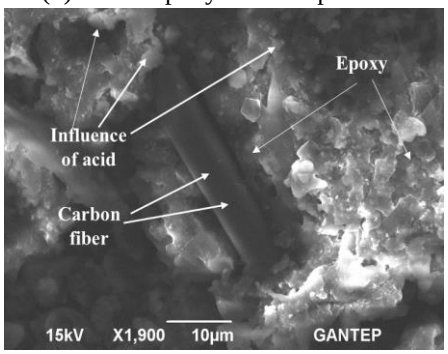

(f) CFRP-epoxy exposed to acid

Fig. 14 SEM pictures of BFRP and CFRP fabric sheets

dimensional instability, cracking, spalling and loss of mechanical performance (Ariffin *et al*. 2013; Bassuoni and Nehdi 2007). As indicated previously, SEM pictures were also taken out of the acid affected zone (indicated as A-1) and less vitreous phases were concentrated on the PVA fibers. SEM results indicated that sulphuric acid attacks started from the outer layer and progressed into the inner side of the specimens. The white deposits also observed in the interfacial transition zone, which deteriorated the bond between PVA fibers and cement matrix. The adverse effect of sulphuric acid on LCFA specimens was lower than the HCFA specimens in both acids affected and unaffected zones.

Fig. 13 presents the SEM pictures of carbon and basalt FRP wrapped HCFA specimens. Results indicated that PVA fibers wrapped with carbon and basalt FRP deteriorated less than unwrapped

PVA fibers in the acidic environment. Due to the sensitivity of the epoxy to the acidic environment, CFRP and BFRP fabrics were also significantly affected by the acid attacks In addition, CFRP wrapped specimens were less influenced compared to BFRP wrapped specimens due to the higher bond between CFRP fabrics and the epoxy as shown in Fig. 14.

4. Conclusions

This study investigates the degradation effect of the sulphuric acid attack on PVA-ECC specimens under static and cyclic loading. The specimens were also reinforced with carbon and basalt FRP fabrics to evaluate performances of the concretes under acid attack. In addition, the FRP material use as a rehabilitation material was also examined. Scanning electron microscopy (SEM) observations were also performed to observe the changes in the surface of PVA fibers and in the interfacial transition zone between the fibers and the matrix. General findings were summarized as follows:

- Visual inspection results indicated that surface color of the high lime containing fly ash (HCFA) specimens changed from grey to white after 15 days of exposure, while the surface color of the low lime fly ash specimens (LCFA) remained grey even after two months of exposure. In addition, more lateral expansion was observed for HCFA specimens.
- LCFA-ECC specimens showed superior durability and mechanical performance than HCFA-ECC specimens. The gypsum and ettringite amount increased due to the high CaO content in HCFA specimens, resulting in the loss of the mechanical performance.
- The incorporation of FRP fabrics into the PVA-ECC specimens improved significantly both compressive strength and ductility. In addition, specimens wrapped with carbon FRP showed better durability and mechanical performance than basalt FRP under both acidic and control environments. The poor performance was observed in unwrapped specimens.
- Specimens wrapped with FRP after the 90-day acid attack indicated that FRP can be used as a rehabilitation material in the acidic environment.
- The connection of the envelopes of the axial stress-strain curve of specimens showed similar behavior under static and cyclic loading. For the post-peak behavior of unwrapped specimens in the acidic environment, the static and cyclic curve separated from each other, especially for HCFA specimens. It may be resulted from the further decrease in elastic modulus under acid attack due to softening of concrete and decreasing the rigidity of the concrete with increasing loading and unloading cycles. For wrapped specimens exposed to both control and acidic environment, FRP showed improved resistance to reversed loadings, the similar stress relaxation behavior was obtained for specimens under both static and cyclic loadings.
- SEM results indicated that sulphuric acid penetration to the specimens started from the surface and progressed to the inward of the cylinder specimens and it deteriorated the bond between PVA fibers and ECC matrix. SEM results also demonstrated that LCFA-ECC specimens were found more durable than HCFA-ECC specimens under sulphuric acid attack. In addition, carbon and basalt FRP specimens showed better durability performance (showed the decreased amount of white deposits) than unwrapped specimens.
- Due to the sensitivity of the epoxy to the acid environment, CFRP and BFRP fabrics are also significantly affected by the sulphuric acid attack. However, due to the existence of the high bond between carbon FRP fabric and the epoxy, CFRP fabrics were less affected than BFRP fabrics by the acid attack.

References

AC125 (1997), Acceptance Criteria for Concrete and Reinforced and Unreinforced Masonry Strengthening Using Fiber-Reinforced Polymer (FRP) Composite Systems, ICC Evaluation Service, Whittier, CA.

ACI Committee 440 (2002), Guide for the Design and Construction of Externally Bonded FRP Systems for Strengthening Concrete Structures (ACI 440.2R-02), Farmington Hills, Mich, American Concrete Institute (ACI).

Al-Tamimia, A., Abed, F.H. and Al-Rahmani, A. (2014), "Effects of harsh environmental exposures on the bond capacity between concrete and GFRP reinforcing bars", *Adv. Concrete Constr.*, **2**(1), 1-11.

Alii, M.R. (2007), "Performance of plain and blended cements exposed to high sulphate concentrations", *Adv. Cement Res.*, **19**(4), 9.

Ariffin, M.A.M., Bhutta, M.A.R., Hussin, M.W., Tahir, M.M. and Aziah, N. (2013), "Sulfuric acid resistance of blended ash geopolymer concrete", *Constr. Build. Mater.*, **43**, 80-86.

ASTM C267-01 (2012), Standard Test Methods for Chemical Resistance of Mortars, Grouts, and Monolithic Surfacings and Polymer Concretes.

ASTM C39/C39M-12 (2012), Standard Test Method for Compressive Strength of Cylindrical Concrete Specimens, 4-2 Annual Book of ASTM Standard, Philadelphia.

Attiogbe, E.K. and Rizkalla, S.H. (1988), "Response of concrete to sulfuric acid attack", *ACI Mater. J.*, **85**(6), 481-488.

Bakis, C.E., Bank, L.C., Brown, V., Cosenza, E., Davalos, J.F., Lesko, J.J. and Triantafillou, T.C. (2002), "Fiber-reinforced polymer composites for construction-State-of-the-art review", *J. Compos. Constr.*, **6**(2), 73-87.

Bassuoni, M.T. and Nehdi, M.L. (2007), "Resistance of self-consolidating concrete to sulfuric acid attack with Consecutive pH Reduction", *Cement Concrete Res.*, **37**, 1070-84.

Cai, J., Pan, J. and Zhou, X. (2017), "Flexural behavior of basalt FRP reinforced ECC and concrete beams", *Constr. Build. Mater.*, **142**, 423-30.

Chaallal, O., Hassan, M. and Shahawy, M. (2003), "Confinement model for axially loaded short rectangular columns strengthened with fiber-reinforced polymer wrapping", *Struct. J.*, **100**(2), 215-221.

Chakrabortty, A. and Khennane, A. (2014), "Failure mechanisms of hybrid FRP-concrete beams with external filament-wound wrapping", *Adv. Concrete Constr.*, **1**, 57-75.

Demers, M. and Neale, K.W. (1994), "Strengthening of concrete columns with unidirectional composite sheets", *Development in Short and Medium Span Bridge Engineering '94, Proc., 4th Int. Conf. on Short and Medium Bridges*, Eds. A.A. Mufti, B. Bakht, and L.G. Jaeger, Canadian Society for Civil Engineering, Montreal.

FBI (2001), "Externally bonded FRP reinforcement for RC structures", International Federation for Structural Concrete, Lausanne, Switzerland.

Halliwell S. (2010), "FRPs-the environmental agenda", *Adv. Struct. Eng.*, **13**(5), 783-91.

Hamilton, H.R., Benmokrane, B., Dolan, C.W. and Sprinkel, M.M. (2009), "Polymer materials to enhance performance of concrete in civil infrastructure", *Polym. Rev.*, **49**(1), 1-24.

Hollaway, L.C. (2001), *Advanced Polymer Composites and Polymers in the Civil Infrastructure*, Elsevier.

Hosseinpour, F. and Abbasnia, R. (2014), "Experimental investigation of the stress-strain behavior of FRP confined concrete prisms", *Adv. Concrete Constr.*, **2**(3), 177-92.

Kumar, S., Sharma, N. and Ray, B.C. (2007), "Acidic degradation of FRP composites", *Proceedings of the the National Conference on Developments in Composites*, India.

Lam, L., Teng, J.G., Cheung, C.H. and Xiao, Y. (2006), "FRP-confined concrete under axial cyclic compression", *Cement Concrete Compos.*, **25**(10), 949-58.

Lau, K.T. and Zhou, L.M. (2001), "The mechanical behaviour of composite-wrapped concrete cylinders subjected to uniaxial compression load", *Compos. Struct.*, **52**(2), 189-98.

Li, V.C. and Fischer, G. (2002), "Reinforced ECC-an evolution from materials to structures", *Concrete Structures in the 21st Century: Proceedings of the First FIB Congress*, Osaka, October.
Li, V.C., Wu, C., Wang, S., Ogawa, A. and Saito, T. (2002), "Interface tailoring for strain-hardening polyvinyl alcohol-engineered cementitious composite (PVA-ECC)", *Mater. J.*, **99**(5), 463-472.
Liu, H., Zhang, Q., Li, V., Su, H. and Gu, C. (2017), "Durability study on engineered cementitious composites (ECC) under sulfate and chloride environment", *Constr. Build. Mater.*, **133**, 171-181.
Meng, D., Huang, T., Zhang, Y.X. and Lee, C.K. (2017), "Mechanical behaviour of a polyvinyl alcohol fibre reinforced engineered cementitious composite (PVA-ECC) using local ingredients", *Constr. Build. Mater.*, **141**, 259-70.
Mesbah, H.A. and Benzaid, R. (2017), "Damage-based stress-strain model of RC cylinders wrapped with CFRP composites", *Adv. Concrete Constr.*, **5**(5), 539-61.
Nanni, A. (1995), "Concrete repair with externally bonded FRP reinforcement", *Concrete Int.*, **17**(8), 22-26.
Nanni, A. and Bradford, N. M. (1995), "FRP jacketed concrete under uniaxial compression", *Constr. Build. Mater.*, **9**, 115-124.
Nazari, A. and Sanjayan, J.G. (2015), "Stress intensity factor against fracture toughness in functionally graded geopolymers", *Arch. Civil Mech. Eng.*, **15**(4), 1007-1016.
Nazari, A., Maghsoudpour, A. and Sanjayan, J.G. (2015), "Flexural strength of plain and fibre-reinforced boroaluminosilicate geopolymer", *Constr. Build. Mater.*, **76**, 207-213.
Pan, Z., Wu, C., Liu, J., Wang, W. and Liu, J. (2015), "Study on mechanical properties of cost-effective polyvinyl alcohol engineered cementitious composites (PVA-ECC)", *Constr. Build. Mater.*, **78**, 397-404.
Photiou, N.K., Hollaway, L.C. and Chryssanthopoulos, M.K. (2006), "Strengthening of an artificially degraded steel beam utilising a carbon / glass composite system", *Adv. Polym. Compos. Struct. Appl. Constr.*, **20**, 11-21.
Qiu, J.S. and Yang, E.H. (2017), "Micromechanics-based investigation of fatigue deterioration of engineered cementitious composite (ECC)", *Cement Concrete Res.*, **95**, 65-74
Reichhold (2009), *FRP Material Selection Guide*, Reichhold, Inc., Triangle Park, NC.
Reis, J.M.L. and Ferreira, A.J.M. (2006), "The effects of atmospheric exposure on the fracture properties of polymer concrete", *Build. Environ.*, **41**, 262-67.
Sahmaran, M., Lachemi, M., Hossain, K.M., Ranade, R. and Li, V.C. (2009), "Influence of aggregate type and size on ductility and mechanical properties of engineered cementitious composites", *Mater. J.*, **106**(3), 308-316.
Sahmaran, M., Li, M. and Li, V.C. (2007), "Transport properties of engineered cementitious composites under chloride exposure", *ACI Mater. J.*, **104**(6), 604-611.
Shah, S.P., Fafitis, A. and Arnold, R. (1983), "Cyclic loading of spirally reinforced concrete", *J. Struct. Eng.*, ASCE, **109**(7), 1695-1710.
Soroka, I. (1979), *Portland Cement Paste and Concrete*, Macmillan Press, London.
Taghia, P. and Bakar, S.A. (2013), "Mechanical behaviour of confned reinforced concrete-CFRP short column- based on finite element analysis", *World Appl. Sci. J.*, **24**(7), 960-970.
Teng, J.G., Chen, J.F., Smith, S.T. and Lam, L. (2002), *FRP-Strengthened RC Structures*, John Wiley & Sons, UK.
Theodoros, R. (2001), "Experimental investigation of concrete cylinders confined by carbon FRP sheets under monotonic and cyclic axial compression load", Research Report 01:2, Division of Building Technology, Chalmers University of Technology.
Thokchom, S. (2014), "Fly ash geopolymer pastes in sulphuric acid", *Int. J. Eng. Innov. Res.*, **3**(6), 943-947.
TR 55 (2004), "Design guidance for stengthening concrete structures using fibre composite materials", The Concrete Society, Camberley, Surrey, England.
Wallah, S.E. and Rangan, B.V. (2006), "Low-calcium fly ash-based geopolymer concrete: long-term properties", *Curtin University*.
Wu, C. and Li, V.C. (2017), "Thermal-mechanical behaviors of CFRP-ECC hybrid under elevated temperatures", *Compos. Part B: Eng.*, **110**, 255-66.
Yang, E.H., Sahmaran, M., Yang, Y.Z. and Li, V.C. (2009), "Rheological control in production of engineered

cementitious composites", *Mater. J.*, **106**(4), 357-66.
Zhang, Z. and Zhang, Q. (2017), "Self-healing ability of engineered cementitious composites (ECC) under different exposure environments", *Constr. Build. Mater.*, **156**, 142-151.

CC